

6 Bunch Compressor and Transfer to Main Linac

6.1 Introduction

The equilibrium bunch length in the damping ring (DR) is 6 mm, too long by an order of magnitude for optimum collider performance ($\sigma_z = 0.3$ mm). Hence the bunch must be compressed longitudinally by a factor of ~ 20 before being injected into the main linac.

Compression is achieved by introducing an energy-position correlation along the bunch length using an RF section, followed by a dispersive beamline with an energy dependent path length: in this way, the tail of the bunch can be made to follow a shorter path than the head, and the bunch becomes shorter. For the dispersive (compressing) beamline, a simple wiggler chicane will be used.

In addition to the bunch compressor, the ring-to-linac transfer line also includes the following sections:

Spin rotator The particle spin orientation in the damping ring must be vertical to preserve the polarisation. To adjust the spin vector to the required orientation at the collision point, a so-called spin rotator is required. The system consists of a combination of dipole and superconducting solenoid magnets.

Coupling correction section The large horizontal to vertical emittance ratio requires a high degree of betatron coupling control. A section containing skew-quadrupoles provides a sufficient empirical correction of the cross-plane coupling.

Diagnostic and collimation section The transfer line includes a diagnostic section which allows continuous monitoring of the beam phase space. The diagnostics serve as a quality control for the complete injection system. For commissioning and tune up a beam dump downstream of the diagnostic section is foreseen. The section also contains the collimators which remove the beam halo before injection into the main linac, decreasing the particle flux at the post-linac collimation system in the beam delivery section, and protecting the accelerating structures in the linac.

Fifteen-degree arc Before injection into the main linac, the TESLA tunnel bends 15° with a 500 meter radius. An achromatic optics is required to transport the large energy spread in the beam ($\sim 3\%$ rms), without causing significant transverse emittance growth.

| | |
|---|-------------------------|
| horizontal emittance $\gamma\epsilon_x$ | 8×10^{-6} m |
| vertical emittance $\gamma\epsilon_y$ | 0.02×10^{-6} m |
| initial bunch length σ_{z_i} | 6×10^{-3} m |
| initial energy spread σ_{δ_i} | 0.13 % |
| beam energy E_0 | 5 GeV |
| final bunch length σ_{z_f} | 0.3×10^{-3} m |
| final energy spread σ_{δ_f} | 2.7 % |
| compression ratio | 20 |

Table 6.2.1: *Beam parameters before and after the TESLA bunch compressor.*

6.2 Bunch Compressor

A detailed description of the bunch compressor can be found in [1]. Here only a brief overview is given.

The first stage of bunch compression is to introduce a longitudinally correlated energy spread in the bunch; this is accomplished by injecting the bunch into an accelerating section at a phase close to the zero-crossing of the RF waveform. The bunch is then compressed by transporting it through a dispersive section, constructed from a series of magnetic chicanes, which provides the necessary path length dependence on energy.

From the conservation of longitudinal emittance, we can immediately write down the final relative (rms) energy spread (σ_{δ_f} , $\delta \equiv \Delta p/p$) of the beam:

$$\sigma_{\delta_f} = \sigma_{\delta_i} \cdot \frac{\sigma_{z_i}}{\sigma_{z_f}},$$

where σ_{z_i} is the initial (DR) bunch length, σ_{z_f} the final (compressed) bunch length, and σ_{δ_i} the initial (DR) rms relative energy spread. Hence the RF must increase the energy spread of the bunch by the same factor as the bunch is compressed (~ 20).

The change in path length (Δl) with energy due to a dispersive beamline is normally expressed as a series expansion:

$$\Delta l = R_{56}\delta + T_{566}\delta^2 + \dots$$

For the coefficients we adopt the matrix convention defined in [2]. For small δ , we can use the linear approximation. For a given bunch compression and associated final energy spread, the required R_{56} is given by

$$R_{56} = \frac{\sqrt{\sigma_{z_i}^2 - \sigma_{z_f}^2}}{\sigma_{\delta_f}}.$$

For a linear compressor, a coefficient $R_{56} \approx 0.22$ m would be required. The basic parameters for the TESLA bunch compressor are given in table 6.2.1 [1].

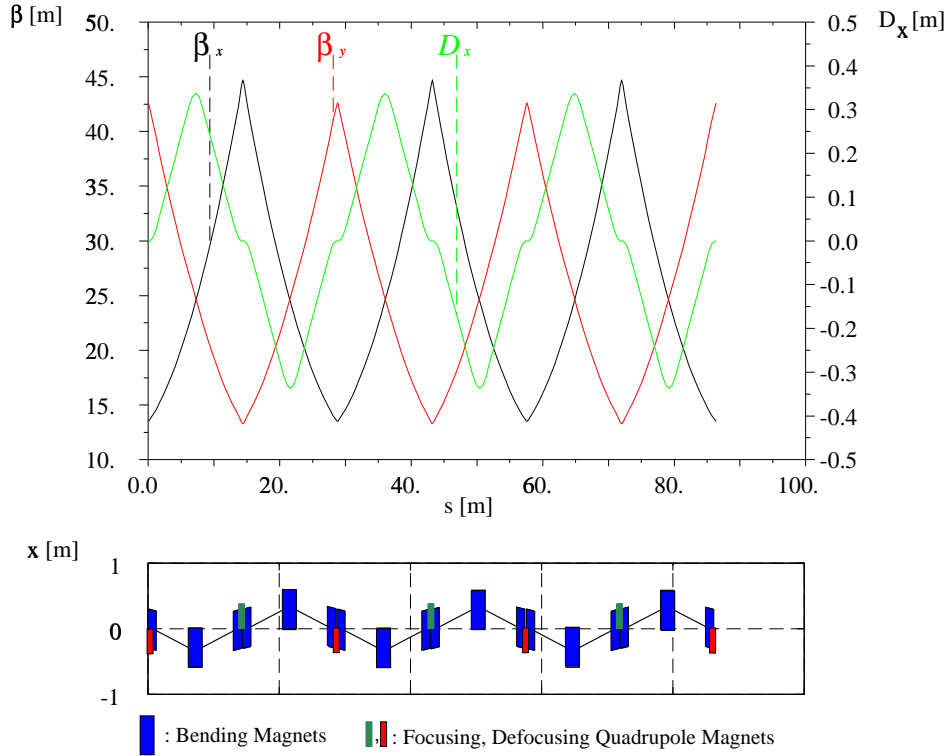


Figure 6.2.1: *Optical functions and floor plan of the wiggler bunch compressor: horizontal (black) and vertical (red) betatron function and horizontal dispersion (green).*

The large rms energy spread of $\sim 3\%$ in the magnetic compression section means that the non-linear terms in the path length (T_{566}) can no longer be ignored. The δ^2 term causes a non-linear deformation of the phase space during compression, which increases the final bunch length. A useful figure of merit is the ratio $r = T_{566}/R_{56}$, which ideally should be made as small as possible.

In addition to the above considerations, the compressor system must not cause any significant transverse emittance growth. There are two mechanisms by which emittance growth can occur:

- chromatic aberrations — most notably non-linear dispersive effects in the horizontal plane — which must be made small owing to the 3% energy spread in the beam;
- the effects of coherent and incoherent synchrotron radiation (CSR and SR respectively), which constrain the strength of the bending magnets and the overall length of the system.

Figure 6.2.1 shows the magnetic wiggler system for the compressor. It consists of bending magnet chicanes (wiggler type) embedded in a FODO structure. No additional

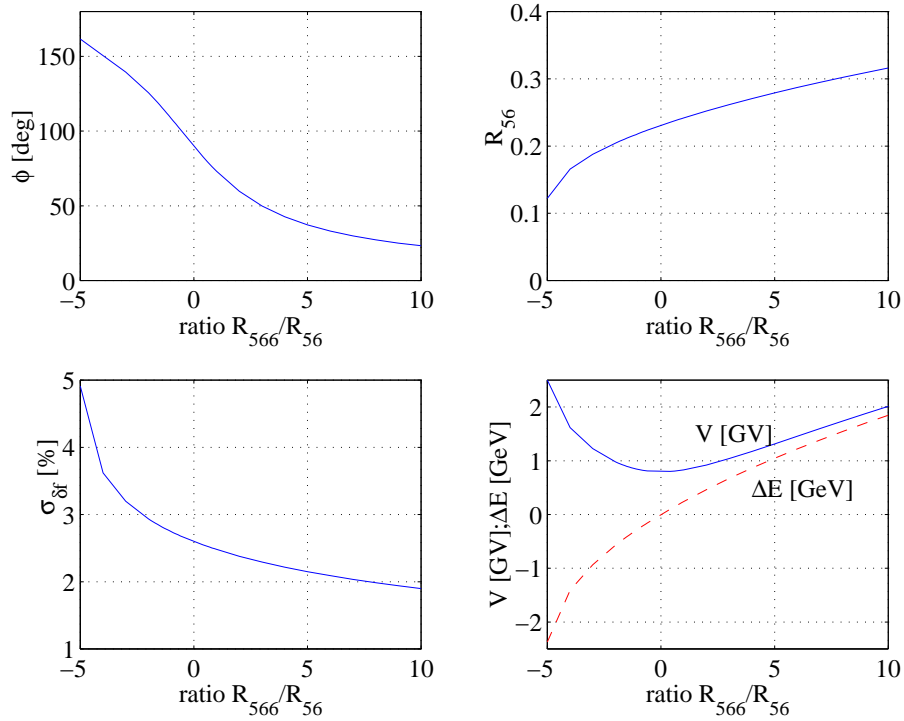


Figure 6.2.2: Accelerating phase (upper left), longitudinal dispersion R_{56} (upper right), final energy spread (lower left), and effective accelerating voltage (lower right) as a function of $r = T_{566}/R_{56}$. The final bunch length is $300 \mu\text{m}$.

optical elements are included between the bending magnets of each individual wiggler section. As a result, the dispersion is zero at every quadrupole, and no higher-order dispersion is generated.

The disadvantage of a wiggler-based system is that the ratio r is fundamentally fixed at a value of $\approx -3/2$, and cannot be influenced by the design parameters. For an energy spread of 3% the value is too large to be left uncorrected, since the non-linear effects would significantly increase the final bunch length.

To compensate the effect of the δ^2 term, we use the curvature of the RF in the upstream accelerator section. By adjusting the phase of the bunch away from the zero-crossing of the RF (i.e. away from the linear slope), a non-linear energy correlation along the bunch length can be introduced. By a careful choice of parameters, this correlation can offset the effects of the non-linear path length in the wiggler section (to second-order in δ). Figure 6.2.2 shows the accelerating phase, gradient, and R_{56} necessary to cancel the second-order terms for various ratios $r = T_{566}/R_{56}$. For a negative value of r as we have here, the beam has to be decelerated on average to achieve the desired correction. Details of the compensation scheme can be found in [1, 3, 4].

The parameters for the wiggler-based compressor are presented in the table 6.2.2. The required peak voltage of the RF before the wiggler is 890 MV at a phase $\phi =$

| | |
|--|---------|
| longitudinal dispersion R_{56} | 0.215 m |
| final energy spread $\sigma_{\delta f}$ | 2.8 % |
| total RF voltage V_{RF} | 890 MV |
| RF phase angle ϕ_{RF} | 113° |
| total chicane length | 86.4 m |
| SR induced emittance growth $\Delta\varepsilon_x/\varepsilon_{x0}$ | 0.02% |

Table 6.2.2: Basic parameters of the wiggler bunch compressor.

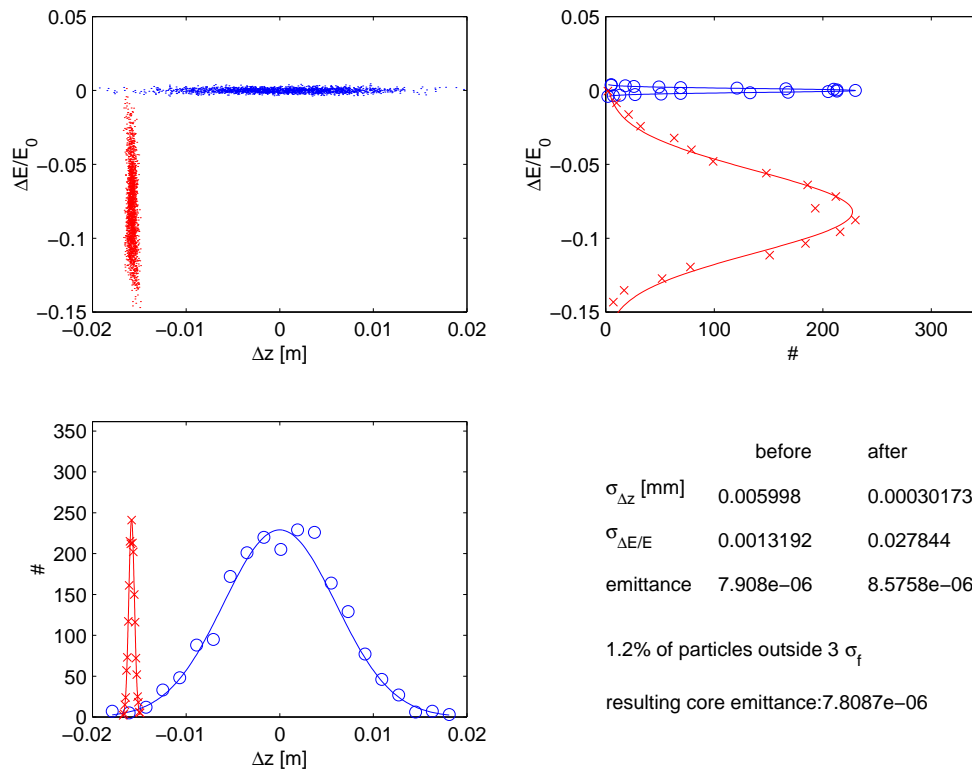


Figure 6.2.3: Longitudinal phase space before (blue) and after (red) the bunch compressor.

113°; this voltage will be provided by three TESLA accelerating modules with an average gradient of 23.8 MV/m. The average energy loss is 0.4 GeV which has to be compensated by two additional accelerating modules. The optimised value of $R_{56} = 0.215$ m reflects a small change from the previous value of 0.22 m due to the non-linear compensation scheme. The total length of the bunch compressor (including three accelerating modules) is ≈ 140 m. The maximum deviation from the central axis is 0.3 m, which should fit easily into the main linac tunnel.

To check the performance of the compressor, six-dimensional particle tracking using the code MAD[5] was performed. Figure 6.2.3 shows the longitudinal phase space before and after the bunch compressor. No significant transverse emittance growth was observed.

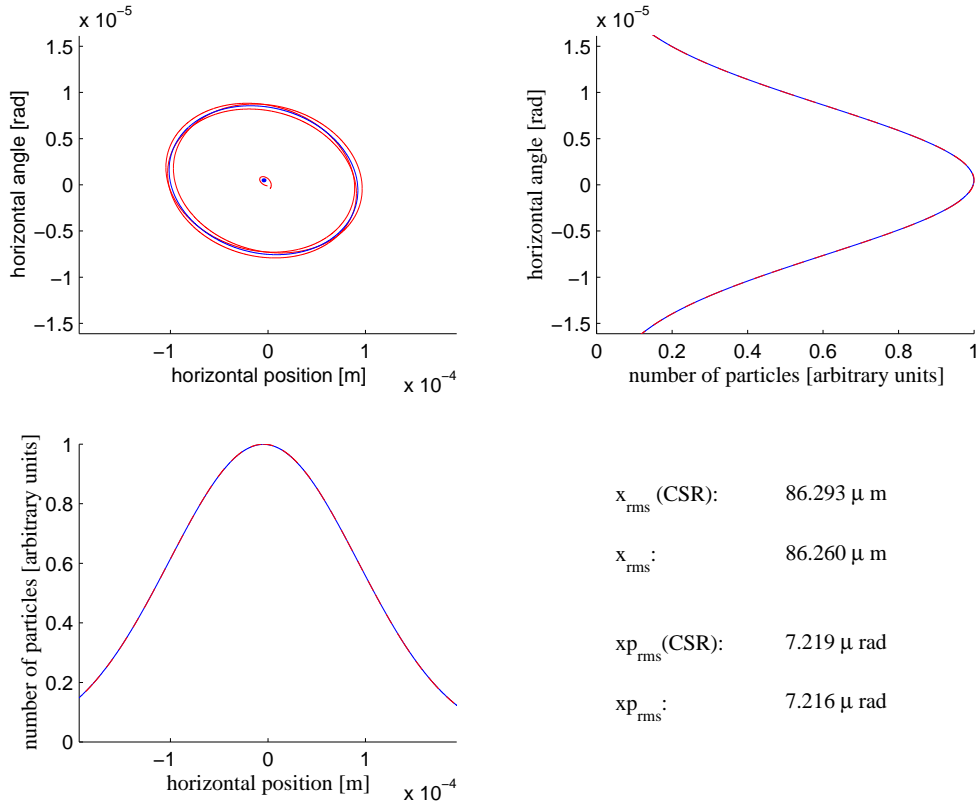


Figure 6.2.4: *TraFiC4*-calculation of emittance growth due to Coherent Synchrotron Radiation effects. Shown are horizontal phase space and projections (red lines/dots: with CSR, blue lines/dots: without CSR). Upper left: horizontal phase space with longitudinal bunch slice centres and 1σ -ellipses. Upper right: projection of particle angles. Lower left: projection of particle positions.

As a final check on the wiggler performance, a calculation of emittance growth due to Coherent Synchrotron Radiation (CSR) effects was made using the code *TraFiC4*[6]. CSR effects cause an emittance growth which is correlated along the bunch length similar to single bunch wakefield effects in the linac. At the compressor exit, the correlated normalised emittance is about 2.5×10^{-7} m, the uncorrelated emittance is preserved and the projected emittance grows by less than 1%. Figure 6.2.4 shows the horizontal phase space and its projections at the end of the compressor.

6.3 Spin Rotator

The spin rotation is constructed from superconducting solenoids and a normal conducting bend section (arc), located upstream of the bunch compressor. A system consisting only of normal conducting vertical and horizontal bending magnets (a so-called ‘half-serpent’ 90° spin rotator) is not an option for TESLA, since long dipoles (~ 150 m) would be required to reduce emittance growth due to synchrotron radiation [7, 8].

| | |
|--|---------|
| longitudinal dispersion R_{56} | 0.005 m |
| maximum spin rotation in solenoid $\nu_{solenoid}$ | 90° |
| total arc bend angle ϕ | 8.0° |
| spin rotation angle in the arc ν_{arc} | 90° |
| total length of rotator system L_{tot} | 85m |
| SR induced emittance growth $\Delta\epsilon_x/\epsilon_{x0}$ | 0.02% |

Table 6.3.1: *Basic spin rotator parameters.*

Since the damped beam is flat ($\epsilon_y/\epsilon_x \ll 1$) the cross-plane coupling induced by the solenoids must be compensated. This is achieved by a spin rotator unit constructed from two identical superconducting solenoids, separated by a short beamline whose (transverse) optics form a $-I$ transformation; this effectively cancels the betatron coupling, while the spin rotation of the two solenoids add. A single unit can rotate the spin around the longitudinal axis by up to 90°. The complete spin rotator is constructed from three sections:

- an initial solenoid pair, which rotates the spin around the local longitudinal (z) axis by $\pm 90^\circ$;
- a normal conducting horizontal arc, which further rotates the spin around the vertical axis by 90°; and
- a final solenoid pair, providing an additional rotation about the z -axis by $\pm 90^\circ$.

With the above combination of rotations, all possible spin orientations can be achieved.

The focusing effect of the solenoids is corrected with four matching quadrupoles per paired solenoid section. The matching quadrupoles are positioned between the solenoid sections and the central arc (see figure 6.5.1). With the solenoids at maximum field strength, the chromatic emittance growth is $\sim 1\%$ ($\sigma_{\delta_i} \approx 0.13\%$). The parameters of the spin rotator system are given in table 6.3.1.

6.4 Auxiliary Beamline Sections

6.4.1 Coupling correction section

In order to empirically correct anomalous cross-plane coupling due to either damping ring extraction or spin rotator errors, a coupling correction section of the type proposed in [9] is included. The system is constructed from four skew-quadrupoles with zero nominal strength. The betatron phase advance between the first and second skew quadrupoles, and the third and fourth skew-quadrupoles is $\Delta\psi_x = \Delta\psi_y = \pi/2$; the second and third are separated by $\Delta\psi_x = \pi, \Delta\psi_y = \pi/2$ such that the four skew quadrupoles orthogonally control the four coupled correlations in the beam: $\langle x'y \rangle$, $\langle xy' \rangle$, $\langle xy \rangle$ and $\langle x'y' \rangle$. Using skew-quadrupoles with a length of 0.1 m, ± 0.1 T pole-tip

field and a 0.01 m pole-tip radius, a factor of about two in emittance increase can be corrected per skew-quadrupole.

6.4.2 Diagnostic and collimation section

A wire-array emittance measurement station [9] is located downstream of the wiggler section. The section is design to continuously monitor the matching and emittance of the beam before being injected into the linac. A wire-array station is constructed from a series of n FODO cells, with a profile monitor (wire¹ scanner) located at each vertically focusing quadrupole ($\hat{\beta}_y$). A minimum of $n = 3$ scanners are required to uniquely determine the emittance of the beam. To add some statistical redundancy, we choose $n = 4$. The optimal phase advance per cell is then given by $\pi/n = \pi/4$.

The nominal rms beam size at the monitors is $5\ \mu\text{m}$ vertically and $70\ \mu\text{m}$ horizontally. A correctly matched beam is easily identified since the beam size (for a single plane) is identical at each of the four wire scanners. The cross-plane coupling can not be accurately determined using this system: however, by simply minimizing the vertical emittance (flat beam) with the four skew-quadrupoles in the upstream coupling correction section, all coupling can be corrected (with some iteration necessary in extreme cases). A direct measurement of the coupled correlations in the beam can be made by using six wire scanners with similar phase advances if necessary [9].

Transverse phase space collimation is obtained by placing four mechanical spoiler pairs in a FODO lattice with appropriate phase advance. Energy collimation is done in the fifteen-degree arc.

6.4.3 Fifteen-Degree Arc

The fifteen-degree arc is necessary to accommodate the special tunnel geometry required for the option of colliding TESLA bunches with HERA proton beams. The arc is constructed from an achromatic lattice with an energy acceptance of $\pm 10\%$. Strong focusing, chromatic correction using sextupole magnets, and small cell length is needed to prevent emittance growth. The bending magnets are vertically focusing (combined function) to maintain sufficient dynamic aperture by reducing the vertical betatron function. Figure 6.4.1 shows the optical functions of one achromatic cell. Figure 6.4.2 shows the results of tracking simulations for a beam with an energy spread of 3% rms. The longitudinal dispersion R_{56} is small (0.002 m) and affects the bunch length by less than 5%.

6.5 Beamline Geometry

Figure 6.5.1 shows the floor plan of the entire tunnel in the electron damping ring extraction and injection region. The floor plan starts at the ‘500 MeV point’, where

¹by wire we refer to either a mechanical wire device or a laser wire.

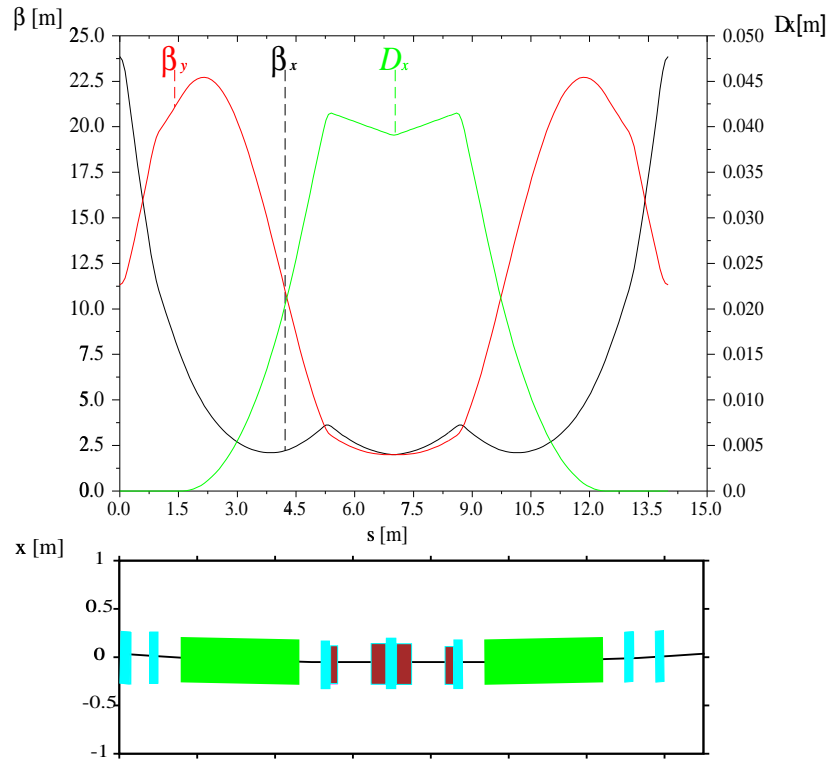


Figure 6.4.1: *Optical functions and floor plan of one achromatic arc cell. Dipoles are green, quadrupoles blue and sextupole magnets are brown.*

the various pre-accelerator linacs deliver the bunch trains for TESLA collider and FEL operation to the 5 GeV electron injector linac (section 4.2).

At the exit of the injector linac, a horizontal dipole pulsed at 5 Hz¹ deflects the collider pulses into a vertical transfer line which then (horizontally) injects the beam into the damping ring. The damping ring is situated about two meters above the main linac axis.

After ~ 200 ms the beam is horizontally ejected from the damping ring, and deflected down to the level of the main linac, where it is injected into the spin rotator and the bunch compressor. This beamline runs parallel to the injector linac. Figure 6.5.2 shows a cross-section of the tunnel. To allow a clear passage, the tunnel monorail (chapter 8) has to move to the side by 0.7 m in the area of the spin rotator.

After passing through the bunch compressor, diagnostics and collimation section and fifteen-degree arc, a second 5 Hz pulsed dipole joins the trajectories of the collider and FEL beams together before they are injected into the main linac.

The positron system is essentially the same as that described above. The geometry

¹The injector linac runs at 10 Hz, alternately accelerating bunches for the collider and the FEL. Only the beam for the collider is injected into the damping ring.

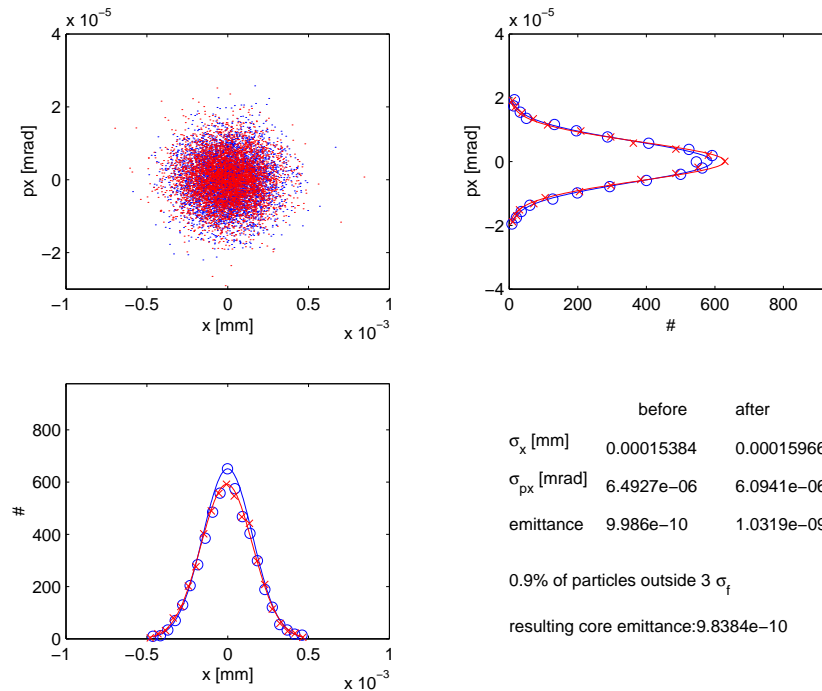


Figure 6.4.2: Horizontal phase space before (blue) and after (red) tracking through the fifteen-degree arc. The rms energy spread of the beam is 3%.

is simplified, however, since the positron injector linac is located at the opposite end of the damping ring (at the high-energy end of the main linac). In addition, there is no FEL beamline and the fifteen-degree arc is not needed.

6.6 Magnet and RF Systems Summary

The complete list of magnets and RF modules (and their specifications) for the entire ring-to-linac transfer line is given in table 6.6.1.

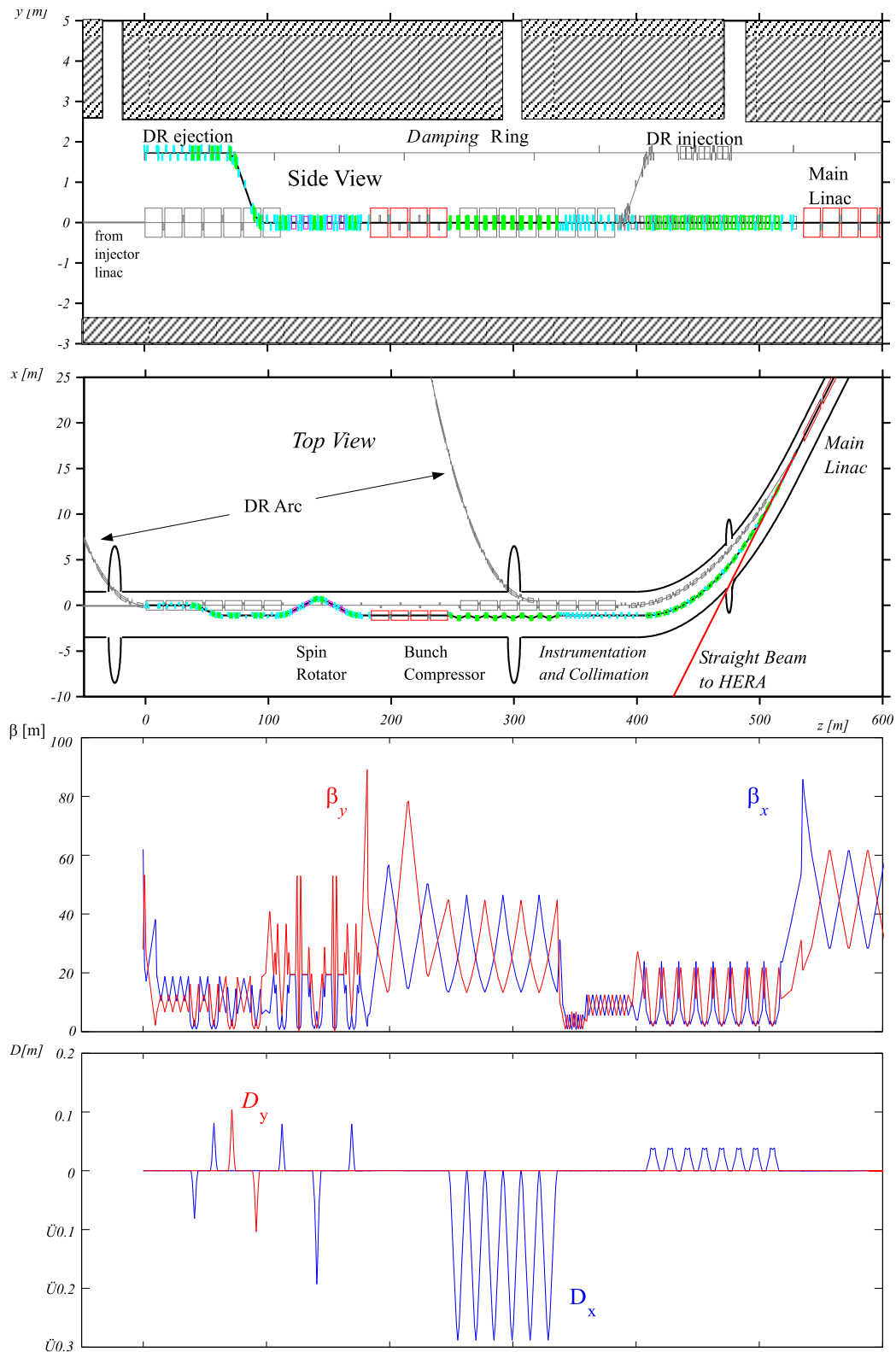


Figure 6.5.1: Floor plan, betatron functions and dispersion for the complete beamline. In the floor plan, bending magnets are green, quadrupoles blue, RF cavities red and solenoid magnets magenta. The damping ring components and those of the injector linac are shaded in grey.

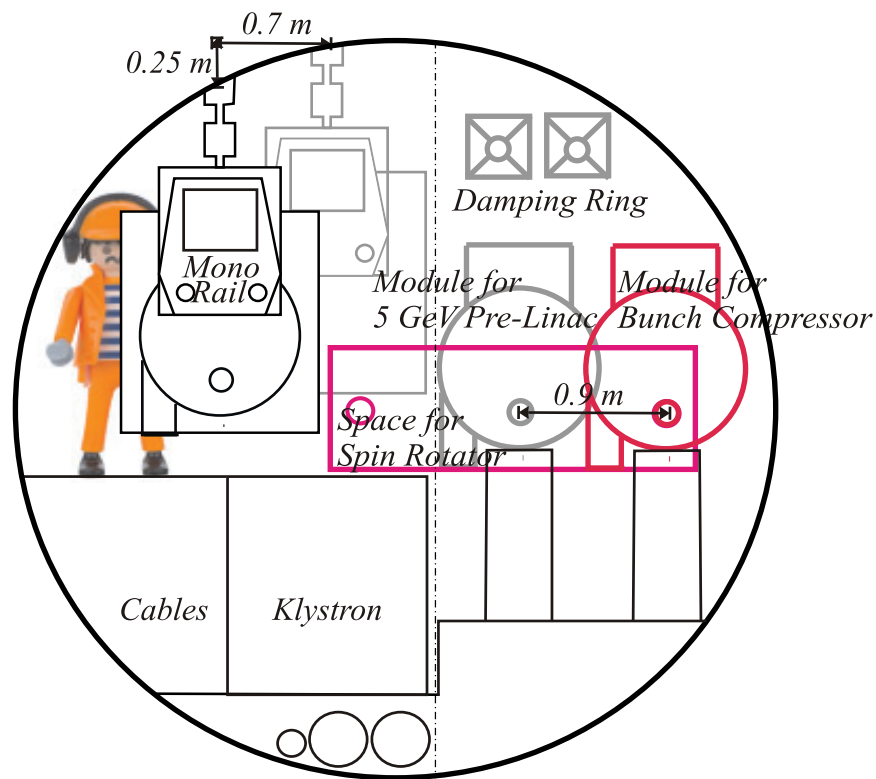


Figure 6.5.2: Cross-section of the TESLA tunnel in the electron damping ring injection/ejection region, looking upstream towards the injector. The RF modules of the two beam lines are interleaved (see figure 6.5.1).

| Bending Magnets | Quantity | Mag. Length [m] | Defl. Angle [deg] | Mag. Field [T] | Gap [mm] |
|-------------------|----------|-----------------|---------------------------------|----------------|----------|
| horizontal dogleg | 4 | 1.0 | 2 | 0.582 | 20 |
| vertical dogleg | 4 | 1.25 | 2.5 | 0.582 | 20 |
| spin rotator | 4 | 0.75 | 2 | 0.776 | 20 |
| | 4 | 1.5 | 4 | 0.776 | 20 |
| bunch compressor | 12 | 1.075 | 3.2 | 0.785 | 20 |
| | 6 | 2.15 | 6.4 | 0.785 | 20 |
| 15 degree arc | 16 | 3.0 | 0.9375 with 2.5 T/m gradient | 0.091 | 20 |

| Quadrupoles | Quantity | Mag. Length [m] | Max. Gradient [T/m] | Bore [mm] |
|-------------|----------|-----------------|---------------------|-----------|
| | 170 | 0.2–0.4 | 25.0 | 20 |

| Sextupoles | Quantity | Mag. Length [m] | Max. Gradient [T/m ²] | Bore [mm] |
|---------------|----------|-----------------|-----------------------------------|-----------|
| 15 degree arc | 32 | 0.4 | 850 | 20 |

| Solenoids | Quantity | Mag. Length [m] | Nom. Field [T] | Bore [mm] |
|--------------|----------|-----------------|----------------|-----------|
| spin rotator | 4 | 3.55 | 3.8 | 20 |

| RF-Modules | Quantity | Number of Cavities | Max. Gradient [MV/m] |
|------------------|----------|--------------------|----------------------|
| bunch compressor | 3 | 12 | 23.8 |

| Correctors | Quantity | Mag. Length [m] | Max. Defl. [deg] | Max. Field [T] | Gap [mm] |
|------------|----------|-----------------|------------------|----------------|----------|
| | 120 | 0.1 | 0.009 | 0.025 | 20 |

Table 6.6.1: *Transfer line magnet parameters.*

Bibliography

- [1] W. Decking, G. Hoffstätter, T. Limberg, *Bunch Compressor for the TESLA Linear Collider*, DESY TESLA-00-40, 2000.
- [2] K. Brown, *A First- and Second-Order Matrix Theory for the Design of Beam Transport Systems and Charged Particle Spectrometers*, SLAC Report-75, 1982.
- [3] P. Emma, *Bunch Compressor Beamlines for the TESLA and S-Band Linear Colliders*, DESY TESLA-95-17, 1995.
- [4] P. Emma, *Bunch Compressor Options for the New TESLA Parameters*, DESY TESLA-98-31, 1998.
- [5] H. Grote and F. Iselin, *The MAD Program*, CERN/SL/90-13(AP), 1996.
- [6] M. Dohlus, A. Kabel and T. Limberg, *Efficient Field Calculation of 3D Bunches on General Trajectories*, Nucl. Instr. Meth. **A445** (2000) 338.
- [7] P. Emma, *A Spin Rotator System for the NLC*, NLC-NOTE 7, 1994.
- [8] T. Fieguth, *Snakes, Serpents, Rotators and the Octahedral Group*, SLAC-PUB-4195, 1987.
- [9] M. D. Woodley, P. E. Emma, *Measurement and Correction of Cross Plane Coupling in Transport Lines*, Proc. 20th Int. Linac Conference, Monterey, CA, Aug. 2000, LINAC2000-MOC19, SLAC-PUB 8581, 2000.